

Fluctuations and Stability of Fisher Waves

Jason Riordan,^{1,*} Charles R. Doering,^{1,2†} and Daniel ben-Avraham^{2,‡}

¹Center for Nonlinear Studies, MS-B258, Los Alamos National Laboratory, Los Alamos, New Mexico 87545

²Department of Physics, Clarkson University, Potsdam, New York 13699-5820

(Received 20 January 1995)

We have performed direct Monte Carlo simulations of the reversible diffusion-limited process $A + A \leftrightarrow A$ to study the effect of fluctuations on a propagating interface between stable and unstable phases. The mean-field description of this process, Fisher's reaction-diffusion equation, admits stable nonlinear wave fronts. We find that this mean-field description breaks down in spatial dimensions 1 and 2, while it appears to be qualitatively and quantitatively accurate at and above 4 dimensions. In particular, the interface width grows $\sim t^{1/2}$ in 1D (exact) and $\sim t^{0.272 \pm 0.007}$ in 2D (numerical).

PACS numbers: 82.20.Mj, 02.70.Lq, 05.90.+m, 82.65.Jv

One of the most well-known theoretical descriptions of the dynamics of invasion of a stable phase into regions of an unstable phase is given by Fisher's reaction-diffusion equation [1,2]. Fisher's equation is

$$\frac{\partial \rho}{\partial t} = D \Delta \rho + k_1 \rho - k_2 \rho^2, \quad (1)$$

where $\rho(\mathbf{x}, t)$ is a local concentration characterizing the state of a system distributed in space ($\mathbf{x} \in \mathbf{R}^d$) and evolving in time. The system under scrutiny is characterized by diffusion coefficient D and positive rate coefficients k_1 and k_2 characterizing the growth and saturation processes described by the local dynamics. Indeed, there are two homogeneous steady states,

$$\rho = 0 \quad (2)$$

and

$$\rho = k_1/k_2, \quad (3)$$

the former being unstable while the latter is stable (boundary conditions permitting, of course).

The invasion process is studied by considering initial conditions consisting of a plane (say, $x_1 = 0$) front separating a stable half space (with $\rho = k_1/k_2$ for $x_1 \leq 0$) from an unstable half space (with $\rho = 0$ for $x_1 > 0$) as illustrated in Fig. 1(a). In the subsequent evolution the front broadens out as the stable density moves into the unstable region, as shown in Fig. 1(b). Although Fisher's equation cannot generally be solved exactly, it can be shown that the wave front approaches a steady, stable wave-front profile $\rho(x_1, \dots, x_d, t) = f(x_1 - ct)$ traveling at constant speed $c \geq c_{\min} = 2\sqrt{k_1 D}$, and satisfying the simple nonlinear ordinary differential equation

$$0 = D \frac{d^2 f(z)}{dz^2} + c \frac{df(z)}{dz} + k_1 f(z) - k_2 f(z)^2. \quad (4)$$

See Fig. 1(c). The minimum speed is realized for initial data with a sharp interface [3].

Fisher's reaction-diffusion equation can be viewed as a mean-field description of the concentration of A -species particles simultaneously undergoing diffusion and the reversible reaction process $A + B \leftrightarrow 2A$, where the

concentration of the B species is in excess or otherwise maintained at a steady level in order to sustain a nonequilibrium state. We refer to Fisher's equation as a mean-field description because the reaction terms are of the form of the mass action rate equation approximation appropriate for systems in local equilibrium, as might be expected for reaction-limited kinetics. The wave-front propagation problem for this system has recently been studied from

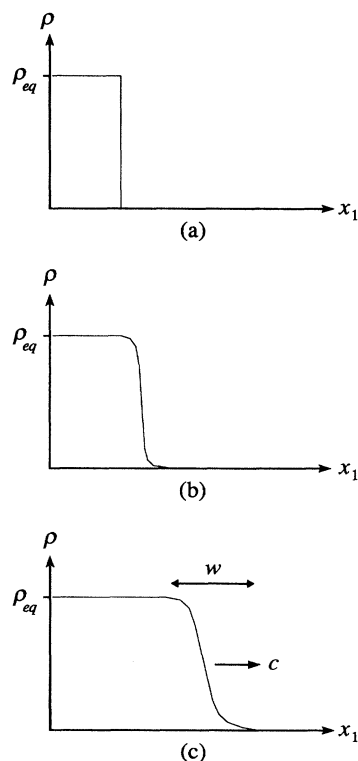


FIG. 1. The invasion process. (a) Initial profile with sharp interface between the stable phase (left) and the unstable phase (right). (b) The wave front begins to broaden as the front moves to the right. (c) The asymptotic wave-front speed is realized, and the wave-front width is w .

the more fundamental microscopic viewpoints of molecular dynamics [4], lattice-gas cellular automata [5], and multivariate master equations [6], though still in a limit of reaction-controlled kinetics in each case.

Within the last decade it has been recognized that the law of mass action breaks down for reaction-diffusion systems in far-from-equilibrium conditions [7], most notably in the diffusion-controlled limit in low spatial dimensions. The $A \leftrightarrow 2A$ reaction (suppressing the role of B , presumed to be held at a steady concentration) has been studied extensively in this regard [8], and in one spatial dimension it has been solved exactly and shown to exhibit a kinetic phase transition in the spatially homogeneous case—a completely new phenomenon outside the realm of the mean-field mass action kinetics [9]. Mean-field kinetics are expected to be valid in high spatial dimensions, even in the diffusion-controlled limit. For example, the concentration of A -species particles for the irreversible coagulation process $2A \rightarrow A$ decays $\sim t^{-1/2}$ in 1D, $\sim t^{-1} \ln t$ in 2D, and $\sim t^{-1}$ in accord with the mean-field rate equation ($d\rho/dt = -k_2\rho^2$) in three and higher dimensions [10]. Thus the critical dimension for the kinetics of the spatially homogeneous irreversible process is two.

The diffusion-controlled wave-front propagation problem has also been solved exactly in one dimension [11]. The exact solution does *not* admit a stable wave front, signaling the qualitative breakdown of Fisher's mean-field picture. The wave-front width w grows with time as $w(t) \sim t^{1/2}$ as the interface propagates in 1D (throughout this paper we refer to the width defined as an *ensemble averaged* width). Stable wave fronts may be expected in high spatial dimensions when the mean-field kinetics take over, so it is natural to wonder about the critical dimension for wave-front propagation.

In this paper we report the results of extensive direct Monte Carlo simulations [12] of the wave-front propagation problem for the diffusion-limited reaction process $A + A \leftrightarrow A$. We find that the wave-front width in 2D grows in time as $w(t) \sim t^{0.272 \pm 0.007}$, while in 4 and higher dimensions the mean-field behavior holds both qualitatively [$w(t) \sim t^0$] and quantitatively [the steady profile shape is well described by Fisher's wave front, the solution to Eq. (4)]. In 3D the data are inconclusive, being equally well fit either by a near-zero exponent or by a logarithmic time dependence. These results indicate that the critical dimension is 3.

The diffusion-limited reaction process $A + A \leftrightarrow A$ on a d -dimensional square lattice with lattice spacing Δx is shown in Fig. 2, where the microscopic rates are defined for the diffusion, birth, and coagulation processes. Sites are either empty or singly occupied. The equilibrium state is a totally random distribution of occupied and unoccupied sites: Balancing the overall birth and coagulation rates as defined in Fig. 2, each site's equilibrium occupation probability is seen to be

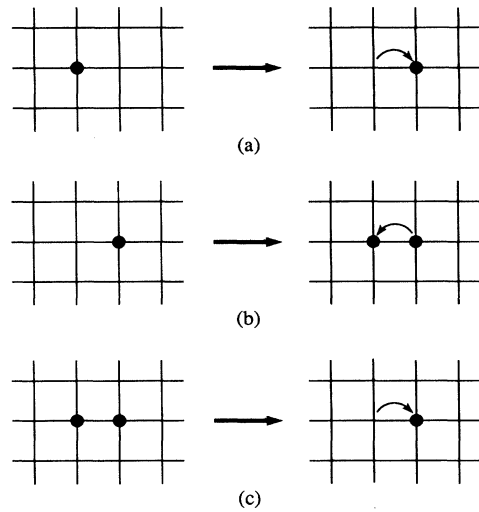


FIG. 2. The rate of the diffusive hopping process, illustrated in (a), is $D/\Delta x^2$, where D is the macroscopic diffusion coefficient. The birth process is shown in (b): Occupied sites spontaneously generate particles at one of 2D neighboring sites at rate $v/2\Delta x$. The coagulation process is demonstrated in (c) where a particle hops onto a neighboring occupied site (at the same hopping rate $D/\Delta x^2$) and the single occupancy rule is enforced, resulting in the net loss of a particle.

$$p_{\text{eq}} = v\Delta x/(2D + v\Delta x). \quad (5)$$

In the simulations with $\Delta x = 1$, rates were chosen to maintain $p_{\text{eq}} = \frac{1}{11}$. Time units in the simulations correspond to $2D = 1$.

The wave-front problem was simulated by considering a long lattice in the x_1 direction ($-L_1 \leq x_1 \leq L_1$) with transverse length $L = L_2 = \dots = L_d$ and periodic boundaries in the x_2, \dots, x_d directions. Initial configurations corresponded to the equilibrium distribution for $x_1 \leq 0$ and an empty lattice for $x_1 > 0$. As the system evolves, the density of particles projected onto the x_1 axis was measured. The simulations were never carried so far that particles were able to reach the $x_1 = L_1$ hyperplane. The front position $X_1(t)$ was computed from the ensemble averaged density projected onto the x_1 axis $\rho(x_1, t)$, according to the discrete version of

$$\begin{aligned} X_1(t) &= \int_{-L_1}^{L_1} x_1 \left(-\frac{1}{\rho_{\text{eq}}} \frac{\partial \rho}{\partial x}(x_1, t) \right) dx_1 \\ &= \frac{1}{\rho_{\text{eq}}} \int_{-L_1}^{L_1} \rho(x_1, t) dx_1 - L_1. \end{aligned} \quad (6)$$

The width was then computed via

$$\begin{aligned} w(t)^2 &= \int_{-L_1}^{L_1} x_1^2 \left(-\frac{1}{\rho_{\text{eq}}} \frac{\partial \rho}{\partial x}(x_1, t) \right) dx_1 - X_1(t)^2 \\ &= \frac{2}{\rho_{\text{eq}}} \int_{-L_1}^{L_1} x_1 \rho(x_1, t) dx_1 - L_1^2 - X_1(t)^2. \end{aligned} \quad (7)$$

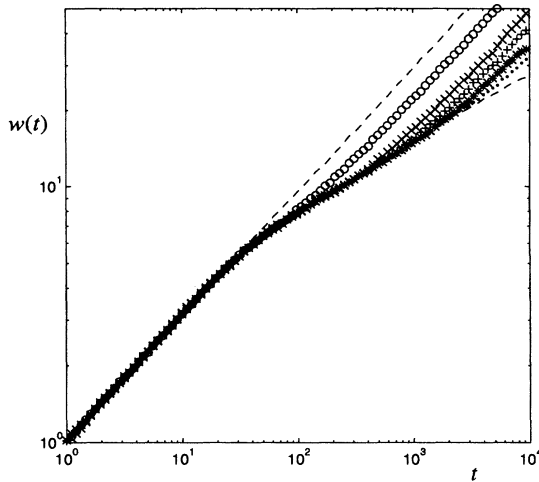


FIG. 3. Raw Monte Carlo data for 2D simulations and transverse systems sizes $L = 4$ (---, top), 16 (\circ), 64 (\times), 128 ($+$), 256 ($*$), 512 (\bullet), and 1024 (---, bottom). All interfaces grow diffusively ($\sim \sqrt{t}$) at early times, crossing over to anomalous scaling near $t = 40$. Then, at a later time which depends on the system size, the scaling crosses back to simple diffusive growth.

These summation expressions for the front position and width are quite effective for providing quality data for these quantities in the face of the inevitable statistical fluctuations inherent in the simulated projected densities.

The raw data for $d = 2$ are plotted in Fig. 3. The finite transverse size L leads to diffusive spreading $\sim t^{1/2}$ at late times, i.e., one-dimensional behavior. (The early time diffusive transient occurs in all dimensions, is independent of system size, and is well described by Fisher's equation due to the lack of correlations in the initial distribution of particles.) At intermediate times a region of nondiffusive wave-front spreading appears, for increasingly long intervals as L is increased. Beyond the early transient, the finite system data is collapsed by invoking the scaling hypothesis [13]

$$w(t) = t^\alpha F(t/L^\beta). \quad (8)$$

Figure 4 is a plot of $w(t)/t^\alpha$ vs t/L^β using the data in Fig. 3 with $\alpha = 0.272$ and $\beta = 1.00$, showing the validity and quality of this assumption. (Error estimates on the exponents $\alpha = 0.272 \pm 0.007$ and $\beta = 1.00 \pm 0.05$ were obtained by varying them until the data separated visibly more than the spread seen in Fig. 4.) Because $F(\xi)$ tends to a constant as $\xi \rightarrow 0$, we conclude that in an infinite system the wave front would continue to spread $\sim t^{0.272 \pm 0.007}$. The wave-front profile achieved a self-similar form in the scaling regime, as shown in Fig. 5.

The raw data for $d = 3$ appeared qualitatively similar to those for $d = 2$, but with a poorer fit by the scaling ansatz in Eq. (8). Hence, other than observing that the data were not inconsistent with a very low exponent

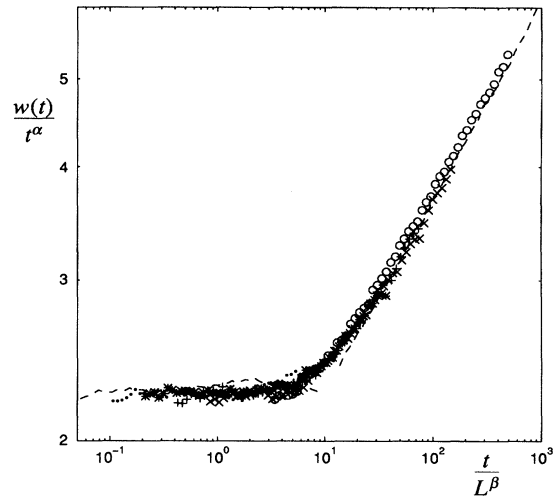


FIG. 4. Collapse of the Monte Carlo data by the scaling hypothesis in Eq. (8), for system sizes $L = 4$ (---, right), 16 (\circ), 64 (\times), 128 ($+$), 256 ($*$), 512 (\bullet), and 1024 (---, left). The 2D simulation data for times $t \geq 50$ are shown. The exponents $\alpha = 0.272$ and $\beta = 1.00$ have been adjusted to achieve the best collapse of the data.

($w \sim t^{0.10}$) or logarithmic ($w \sim \sqrt{\ln t}$) scaling, we are reluctant to draw a quantitative conclusion.

The data for $d = 4$ are well described by the mean-field value $\alpha = 0$, as illustrated in Fig. 6, where several profiles at different times (simulated at transverse size $L = 32$) are seen to collapse with no adjustment to the width. Moreover, mean-field theory provides an excellent

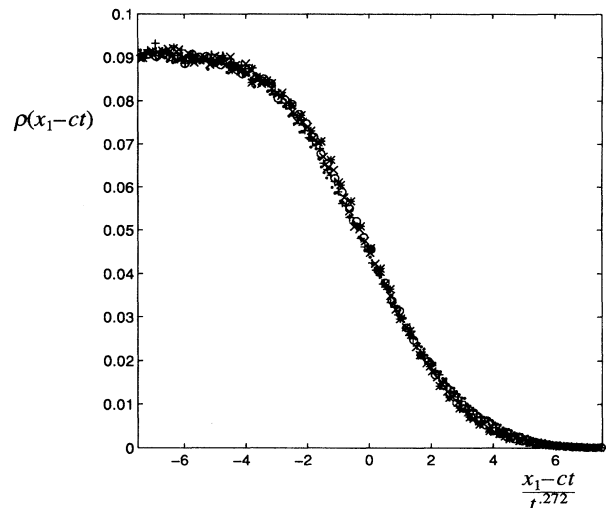


FIG. 5. Rescaled 2D wave-front profiles in the moving frame, illustrating the successful collapse of the wave fronts using the width growth exponent $\alpha = 0.272$. These are the data for the simulation with $L = 1024$, at times $t = 65.31 \times (3.300)^n$, $n = 0$ ($*$), 1 (\circ), 2 (\times), 3 ($+$), and 4 (\bullet).

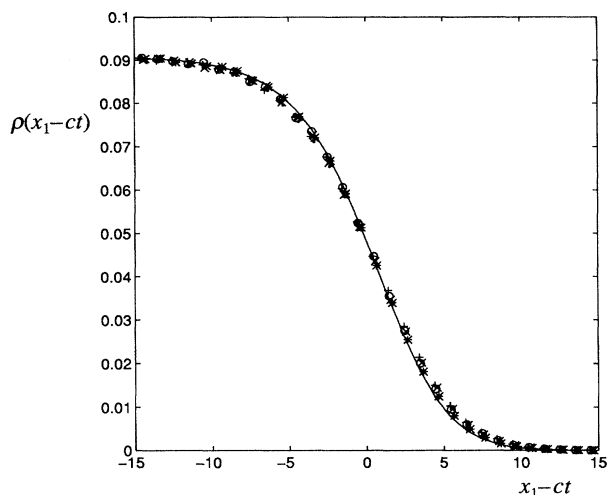


FIG. 6. 4D wave-front profiles in the moving frame, illustrating the successful collapse of the wave fronts using the mean-field width growth exponent $\alpha = 0$. These are the data for the simulation with $L = 32$, at times $t = 43.87 \times (1.348)^n$, $n = 0$ (*), 1 (o), 2 (x), 3 (+), and 4 (•). The solid line is the stationary discrete space mean-field profile using no adjustable parameters.

description of the profile: The spatially discrete version of Eq. (1), projected onto the inhomogeneous direction with mean-field rate coefficients, is

$$\frac{dp_n}{dt} = A[p_{n+1} - 2p_n + p_{n-1}] + [p_{n+1} + 2(d-1)p_n + p_{n-1}][B - Cp_n], \quad (9)$$

with

$$A = \frac{D}{\Delta x^2}, \quad B = \frac{\nu}{2\Delta x}, \quad C = \frac{D}{\Delta x^2} + \frac{\nu}{2\Delta x}, \quad (10)$$

where p_n is the marginal occupation probability of the n th site on the x_1 axis. The steady-state profile in Fig. 6 (solid line) is computed from this discrete space mean-field theory with no adjustable parameters. (The wave fronts are seen to broaden slightly as time evolves, reflecting the approaching finite-size crossover back to diffusive spreading.)

This study is complementary to recent research on directed interface growth and roughening [13,14]. Models of directed interface growth, studied both via Monte Carlo simulations of lattice models and renormalization-based theory of hydrodynamic equations, yield different interface growth exponents than those reported here. At first this may appear surprising. The particular point of departure of the interface growth mechanisms has yet to be identified, but the fundamental differences between externally imposed, anisotropic growth and the

isotropic autocatalytic process studied here suggest that these features may define alternative universality classes.

It will be interesting to see if the nonequilibrium interface growth process in diffusion-limited $A + A \leftrightarrow A$ reported here is contained in a closure approximation to the exact hierarchy of joint distribution evolution equations. Closures, which can be thought of as “improved” mean-field theories, have been shown to qualitatively and quantitatively capture some aspects of the anomalous kinetics of diffusion-limited reactions [15].

We gratefully acknowledge helpful discussions with Z. Rácz, S. Redner, and R. Zia. This research was supported by DOE and NSF (including an REU supplement).

*Electronic address: jay@cmls.lanl.gov

†To whom correspondence should be addressed. Electronic address: doering@cmls.lanl.gov

‡Electronic address: qd00@craft.camp.clarkson.edu

- [1] R. A. Fisher, *Ann. Eugenics* **VII**, 355 (1936).
- [2] A. Kolmogorov, I. Petrovsky, and N. Piskounov, *Bull. Univ. Moskau Ser. Internat. Sec. A* **1**, 1 (1937).
- [3] D. Aronson and H. Weinberger, *Adv. Math.* **30**, 33 (1978); J. D. Murray, *Mathematical Biology* (Springer, Berlin, 1989); G. Gaquette, L.-Y. Chen, N. Goldenfeld, and Y. Oono, *Phys. Rev. Lett.* **72**, 76 (1994).
- [4] A. Lemarchand, H. Lemarchand, E. Sulpice, and M. Mareschal, *Physica (Amsterdam)* **188A**, 277 (1992).
- [5] D. Gruner, R. Kapral, and A. Lawniczak, *J. Chem. Phys.* **99**, 3938 (1993); A. Lemarchand, A. Lesne, A. Perera, M. Moreau, and M. Mareschal, *Phys. Rev. E* **48**, 1568 (1993).
- [6] H. Breuer, W. Huber, and F. Petruccione, *Physica (Amsterdam)* **73D**, 259 (1994).
- [7] K. Kang and S. Redner, *Phys. Rev. A* **32**, 435 (1985); R. Kopelman, *Science* **241**, 1620 (1988).
- [8] D. ben-Avraham, M. Burschka, and C. R. Doering, *J. Stat. Phys.* **60**, 695 (1990); W. Horsthemke, C. R. Doering, T. S. Ray, and M. A. Burschka, *Phys. Rev. A* **45**, 5492 (1992).
- [9] M. Burschka, C. R. Doering, and D. ben-Avraham, *Phys. Rev. Lett.* **63**, 700 (1989); C. R. Doering and M. Burschka, *Phys. Rev. Lett.* **64**, 245 (1990).
- [10] M. Bramson and D. Griffeath, *Ann. Prob.* **8**, 183 (1980); M. Bramson and J. Lebowitz, *Phys. Rev. Lett.* **61**, 2397 (1988).
- [11] C. R. Doering, M. A. Burschka, and W. Horsthemke, *J. Stat. Phys.* **65**, 953 (1991).
- [12] D. ben-Avraham, *J. Chem. Phys.* **88**, 941 (1988).
- [13] M. Plischke and Z. Rácz, *Phys. Rev. A* **32**, 3825 (1985).
- [14] M. Kardar, G. Parisi, and Y. Zhang, *Phys. Rev. Lett.* **56**, 889 (1986); M. Plischke, Z. Rácz, and D. Liu, *Phys. Rev. A* **35**, 3485 (1987).
- [15] J.-C. Lin, C. R. Doering, and D. ben-Avraham, *Chem. Phys.* **146**, 355 (1990); J.-C. Lin, *Phys. Rev. A* **44**, 6706 (1991).